

# Compact modeling of organic thin film transistors with solution processed octadecyl substituted tetrabenzotriazaporphyrin as an active layer

Juan A. Jiménez Tejada, *Member, IEEE*, Pilar López Varo, *Student Member, IEEE*, Andrew N. Cammidge, Isabelle Chambrier, Michael J. Cook, Nandu B. Chaure and Asim K. Ray

**Abstract**—Using 70nm thick spin-coated film of newly synthesized octadecyl substituted copper tetrabenzotriazaporphyrin (10CuTBTAP) as an active layer on a highly doped silicon (110) gate electrode substrates, output characteristics and transfer characteristics of bottom-gate bottom-contact organic thin film transistors have been measured at room temperature. A compact model for thin film transistors has been employed as a part of circuit design tool to extract device parameters such as the charge carrier mobility  $\mu$ , the threshold voltage  $V_T$  and the contact resistances. Parallel measurements and analysis were performed on similarly constructed devices with a copper phthalocyanine analogue (10CuPc). The results reveal that the 10CuPc layer is relatively more susceptible to trapping degradation near the gate region than a 10CuTBTAP layer, which is significant in order to achieve stability in these transistors. The application of the simple square law in the classical MOS model provides a quicker but approximate interpretation of the transistor performance without providing information on the gate voltage dependence of mobility and the effects of the contact regions. In this comparative study, the analysis of the contact regions is found to be very important for determining the difference in the performance of two transistors.

**Index Terms**—Phthalocyanine, MOS, Field effect, Device parameters, Contact effects.

## I. INTRODUCTION

THE field of organic thin film transistors (OTFT) has stimulated intense research interest for their low cost potential applications in large area displays and sensors [1], [2].

Organic materials that are useful for these techniques are generally aromatic compounds [3], [4]. Our particular research

This work was partially supported by Ministerio de Educacin y Ciencia under research Grant FPU12/02712 and MINECO under research Project MAT2016-76892-C3-3-R. Experimental work was carried out at Queen Mary, University of London under financial support from the UK Technology Strategy Board (Project No: TP/6/EPH/6/S/K2536J). The pre-patterned transistor substrates were prepared by QUDOS Technology, Rutherford Appleton Laboratory, Didcot, UK. The authors are grateful to Dr Craig E. Murphy and Dr Markys G. Cain of the National Physical Laboratory, Hampton Road, Teddington, Middlesex UK for fruitful discussions.

J.A. Jiménez Tejada, and P. López Varo are with the Departamento de Electrónica y Tecnología de los Computadores, CITIC-UGR, Universidad de Granada, Granada 18071, Spain; (e-mail: tejada@ugr.es, pilarlopez@ugr.es, respectively).

A. N. Cammidge, I. Chambrier and M. J. Cook are with the School of Chemistry, University of East Anglia, Norwich, NR4 7TJ, UK; (e-mail: a.cammidge@uea.ac.uk, i.fernandes@uea.ac.uk and m.cook@uea.ac.uk, respectively).

N. B. Chaure and A. K. Ray are with the Materials Research Centre, Queen Mary, University of London, Mile End Road London, E1 4NS, UK; (e-mail: n.chaure@physics.unipune.ac.in, and asim.ray@brunel.ac.uk, respectively).

Manuscript received December 1, 2016;

utilizes metallated phthalocyanines that bear eight aliphatic chains that promote solubility in spreading solutions used for thin film formulations [5], and is more recently expanded following our convenient synthesis of closely related structures where one or more of the ring nitrogen atoms are replaced by carbon atoms [6]. This therefore extends the range of compounds available. Elsewhere, Shimizu, Ozaki and coworkers [7] reported beneficial properties of one of these compounds, a metal-free octahexyl substituted tetrabenzotriazaporphyrin, 6H<sub>2</sub>TBTAP for high performance small molecule solar cells and also utilized the range of related compounds in which ring nitrogens were replaced systematically by carbon atoms [8]. Metal phthalocyanines and TBTAP derivatives are photosensitive materials. In PdPc phototransistors, a high increase of the photosensitivity ( $I_{illum}/I_{dark}$ ) has been observed studying the effect of the contacts [9]. The study of their electrical characteristics is thus necessary. The characteristics of bottom-gate bottom-contact OTFTs with 70 nm thick films of solution processed 6NiTBTAP and its phthalocyanine analogue, 6NiPc, as active layers on silicon substrates has been recently reported [10]. They found, on the basis of the classical square law analysis, that the 6NiTBTAP films exhibit superior characteristics in terms of greater saturation of hole mobility, higher on/off ratios and lower threshold voltage.

The analysis of the output characteristics of transistors with the ideal MOS model is widely spread among researchers as it provides a quick picture of the transistor performance. Nevertheless, significant efforts have been spent in recent years to include the charge transport in organic semiconductor, which is clearly different from the transport in crystalline semiconductors, and is usually modeled with a gate-voltage dependent mobility [11], [12], [13], [14], [15]. They can also include detrimental effects produced by the contact region of the organic transistors [16], [17], [18], [19]. These models are also associated with methods to extract their respective parameters from the output characteristics of a transistor.

In this work, we compare the electrical performance of two OTFTs fabricated with octadecyl substituted copper tetrabenzotriazaporphyrin (10CuTBTAP) and copper phthalocyanine analogue (10CuPc) (Figure 1). A compact model is employed for the analysis of the current-voltage characteristics of OTFTs, which includes the effects of the contact regions and an electric field dependent mobility [20]. This compact model is accompanied with a parameter extraction method for the model parameters and the drain-current vs. contact-voltage

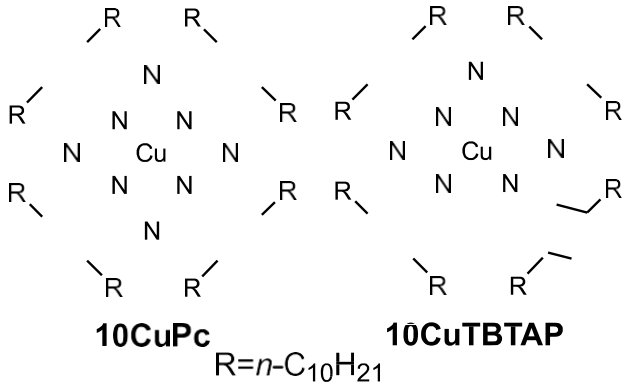


Fig. 1. Active semiconducting materials analyzed in the work: a copper phthalocyanine bearing eight decyl chains, 10CuPc, and a similarly substituted copper tetraazabenzotriazaphyrin denoted as 10CuTBTAP.

$(I_D - V_C)$  curves. **Apart from extracting these curves, the analysis of the evolution of the  $I_D - V_C$  curves at the contact with the applied gate voltage provides a way to detect local non-uniformities such as traps. This kind of characterization is very important in OTFTs in order to analyze the device stability, one of the main challenges in organic devices.** Brief descriptions of device fabrication and measurement techniques are given in Section II. In Section III, we describe the tools that are used to characterize the OTFTs:

(a) a proper model for the output characteristics  $I_D - V_D$  of a transistor, (b) a proper model for the current-voltage characteristic in the region close to the contact,  $I_D - V_C$ , and its incorporation in the output characteristics model, and (c) an extraction method of the  $I_D - V_C$  curves at the contact and the rest of the model parameters out of the resulting combined model. Finally, the results of the comparative study are discussed in Section IV.

## II. EXPERIMENTAL METHODS

Bottom-gate, bottom-contact OTFTs were fabricated on octadecyltrichlorosilane treated 250nm thick  $\text{SiO}_2$  gate insulator on the highly doped (resistivity 1 to 5  $\Omega\text{cm}$ ) Si (110) substrate. 70 nm thick spin-coated films of the two macrocyclic compounds 10CuTBTAP and 10CuPc were used as the active semiconductor layer onto photolithographically pre-patterned 200nm thick gold source-drain electrodes in an interdigitated configuration with channel length  $L = 5 \mu\text{m}$  and channel width  $w = 2 \text{mm}$ . The full protocols of the substrate cleaning, electrode deposition and surface passivation were given in a previous publication [5]. The electrical measurements were performed at room temperature in air under ambient conditions using a Keithley 4200 semiconductor parameter analyzer.

## III. RESULTS

The comparative study of the two transistors under test is initiated with a brief analysis of their output characteristics with the classical MOS model. This is done with the aim of highlighting the importance of using a proper model for TFTs. The output characteristics of the 10CuPc and 10CuTBTAP OTFTs are represented with symbols in Figure 2(a) and (b),

respectively. A first estimation of the values of the carrier mobility and the threshold voltage of these transistors can be obtained with the ideal MOS model:

$$I_D = -k[(V_G - V_T)V_D - V_D^2/2], V_D < V_G - V_T \quad (1)$$

$$I_D = -k(V_G - V_T)^2/2, V_D \geq V_G - V_T$$

where the source terminal is assumed grounded,  $V_G$  is the gate-terminal voltage,  $V_D$  is the drain-terminal voltage or voltage drop between the drain and the source terminals,  $k = wC_i\mu/L$ , and  $C_i$  is the capacitance per unit surface of the oxide,  $C_i = 14 \text{ nF/cm}^2$ . The values of  $k$  and  $V_T$  can be extracted from the  $I_D - V_D$  curves in the saturation regime at  $V_D = -45 \text{ V}$  by using (1). The result is  $k = 6.7 \times 10^{-12} \text{ A/V}^2$ ,  $\mu = 1.2 \times 10^{-6} \text{ cm}^2/\text{Vs}$  and  $V_T = 67 \text{ V}$  for the 10CuPc OTFTs and  $k = 1.7 \times 10^{-11} \text{ A/V}^2$ ,  $\mu = 3.1 \times 10^{-6} \text{ cm}^2/\text{Vs}$  and  $V_T = 39 \text{ V}$  for the 10CuTBTAP OTFTs. Introducing these values in (1), the solid lines in Figure 2 are obtained. From the comparison of experimental data and the numerical calculation, it is clear that values of these parameters are abnormal, only the experimental values in the saturation are reproduced with the ideal MOS model. The triode region is clearly affected by other effects not included in the ideal model, such as the effect of the contacts. The applied voltage between the drain and source terminals  $V_D$  can be split in the voltage drop along the intrinsic channel  $V_{DS}$  plus the voltage drop along the contact region  $V_S \equiv V_C$  (Figure 2(d) in [20]). The extracted threshold voltage is heavily influenced by the contact effects. A simple estimation of an average value for the contact voltage  $\langle V_S \rangle$  can be done by modifying the value of the threshold voltage and maintaining the previous values of  $k$  in order to fit the linear region. If we use in (1) the value  $V_T = V_T^* - \langle V_S \rangle$  where  $V_T^*$  is the value of the threshold value of each transistor obtained above and  $\langle V_S \rangle$  is an average value of the contact voltage ( $\langle V_S \rangle = -50 \text{ V}$  for the 10CuPc OTFT and  $\langle V_S \rangle = -7 \text{ V}$  for the 10CuTBTAP), the result is seen in dashed lines in Figure 2.

With this modification of the threshold voltage, the ideal model (1) reproduces the triode region but not the rest of the output characteristics. Thus, a model that incorporates the effect of the contacts and a non constant mobility is necessary [11], [21], [22]. We use a generic charge drift model [11] which includes the voltage drop at the source contact ( $V_S \equiv V_C$ ) and an electric field dependent mobility  $\mu = \mu_o(V_G - V_T)^\gamma$ :

$$\frac{I_D}{k_o} = -\frac{[(V_G - V_T - V_S)^{\gamma+2} - (V_G - V_T - V_D)^{\gamma+2}]}{\gamma + 2}$$

$$k_o = \mu_o C_i w / L \quad (2)$$

where  $\gamma$  is the mobility enhancement factor,  $k_o = wC_i\mu_o/L$  and  $\mu_o$  is the mobility-related parameter, its dimension is expressed as  $\text{cm}^2/(\text{V}^{1+\gamma}\text{s})$ . In order to provide a single value for the voltage dependent mobility, the mobility is evaluated at  $V_{GT} = V_G - V_T = 1 \text{ V}$  [11], thus  $\mu(V_{GT} = 1 \text{ V}) = \mu_o$  in  $\text{cm}^2/(\text{Vs})$  or  $k(V_{GT} = 1 \text{ V}) = k_o$  in  $\text{A/V}^2$ . This model reflects the fact that the voltage drop at the drain contact is small in comparison to the voltage drop at the source contact [23].

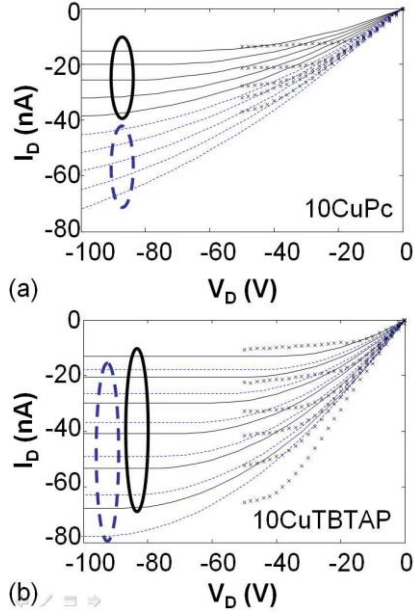


Fig. 2. Comparison of output characteristics measured at different gate voltages  $V_G$  in (a) 10CuPc and (b) 10CuTBTAP OTFTs ( $\times$ ) with the ideal MOS model (lines).  $V_G$  is swept from 0 to -40 V with a -10 V step in (a) and from 0 to -50 V with a -10 V step in (b).  $\mu = 1.2 \times 10^{-6} \text{ cm}^2/\text{Vs}$  and  $V_T = 67 \text{ V}$  (solid lines) or  $V_T = (67 + 50) \text{ V}$  (dashed lines) for the 10CuPc OTFTs.  $\mu = 3.1 \times 10^{-6} \text{ cm}^2/\text{Vs}$  and  $V_T = 39 \text{ V}$  (solid lines) or  $V_T = (39 + 7) \text{ V}$  (dashed lines) for the 10CuTBTAP OTFTs.

Also, this method is especially useful when combined with a characterization technique to extract its parameters. This is the so called  $H_{V_G}$  function [11], [24], defined as:

$$H_{V_G}(V_G) = \int_{<V_T}^{\cdot} I_D(V_G) dV_G / I_D(V_G). \quad (3)$$

The  $H_{V_G}$  function can be evaluated in the linear and saturation modes. In the saturation mode,  $H_{V_G}$  is linear with  $V_G$  [12]:

$$H_{V_G}(V_G) = (V_G - V_T - V_S) / (\gamma + 3) \quad (4)$$

**In the derivation of the function  $H_{V_G}$  in the saturation regime (4), the drain current  $I_D$  (2) is introduced in (3). For simplicity and characterization purposes, the value of the contact voltage  $V_S$  is assumed constant (although  $V_S$  is a function of  $I_D$  and  $V_G$ ,  $V_S = V_S(I_D, V_G)$ ). An appropriate value for  $V_S$  to be used in (4) could be the average value of the contact voltage evaluated over the different gate voltages and drain currents  $V_S \approx \langle V_S \rangle = \langle V_S(I_D, V_G) \rangle$ . The relation  $V_S(I_D, V_G)$  can be extracted from experimental data and (2) if the parameters  $\gamma$ ,  $k_o$  and  $V_T$  are known:**

$$V_S = V_G - V_T - [I_D(\gamma + 2) / k_o + (V_G - V_T - V_D)^{\gamma+2}]^{1/(\gamma+2)} \quad (5)$$

As the relation  $V_S(I_D, V_G)$  is not known a priori, an initial estimation for  $V_S \approx \langle V_S \rangle$  must be provided. In previous works [20], [25], [26], we proposed a method to

extract from experimental ( $I_D - V_D$ ) curves the parameters of this model (2) and the voltage drop at the contact  $I_D - V_S$ . **The method begins with the initial estimation of  $V_S$  in order to extract  $V_T$  and  $\gamma$  from (4).** Once  $V_T$  and  $\gamma$  are determined from (4), the value of  $k_o$  is still unknown. Thus, different values of  $k_o$  are tested and introduced in (5) to find the relation  $V_S - I_D$ . The way to know whether the set of values for the OTFT parameters is correct is by inspecting this relation  $V_S - I_D$ . This relation must make physical meaning, and the average value of the contact voltage obtained from this relation  $V_S - I_D$  must be consistent with the initial guess value of  $\langle V_S \rangle$ . Otherwise, a new value of the average of  $V_S$  must be inserted in (4) and the process must be repeated until these conditions are fulfilled.

It is observed experimentally that output characteristics measured in OTFTs with contact effects show linear or quadratic behaviors at low drain voltages [18], [25]. Therefore, the  $I_D - V_S$  relation can be approximated by the respective relations:

$$V_S = I_D R_C \quad (6)$$

$$I_D = M_C V_S^2 \quad (7)$$

They are simple expressions as they depend only on one parameter,  $R_C$  or  $M_C$ . These expressions are theoretically justified by a previously proposed model that considers injection and transport of charge in organic diodes [19], [27], [28], [29]. In the cases analyzed in Figure 2, a linear trend is observed in the triode region. Thus, a linear  $I_D - V_S$  relation should be obtained after introducing in (5) the experimental data and the proper values of  $V_T$ ,  $\gamma$ ,  $V_S$  and  $k_o$ .

This method is applied to the  $H_{V_G}$  function extracted from transfer characteristics measured in the 10CuPc and 10CuTBTAP OTFTs at  $V_D = -45 \text{ V}$  (crosses in Figure 3). After fitting the experimental  $H_{V_G}$  function with (4), the following values result:  $V_T + V_S = 18 \text{ V}$  and  $\gamma = 1.5$  for the 10CuPc OTFT and  $V_T + V_S = 23 \text{ V}$  and  $\gamma = 1.6$  for the 10CuTBTAP case. Then, the values of the parameters  $V_S$  and  $k_o$  are iteratively modified and introduced in (5) until linear  $I_D - V_S$  curves are obtained. The result is represented with crosses in Figure 4 using the values (a)  $V_T = 38 \text{ V}$ ,  $V_S = -20 \text{ V}$ ,  $k_o = 4.0 \times 10^{-13} \text{ A/V}^2$ ,  $\mu_o = 7.2 \times 10^{-8} \text{ cm}^2/\text{Vs}$  and  $\gamma = 1.5$  for the 10CuPc OTFT and (b)  $V_T = 43 \text{ V}$ ,  $V_S = -20 \text{ V}$ ,  $k_o = 1.2 \times 10^{-13} \text{ A/V}^2$ ,  $\mu_o = 2.2 \times 10^{-8} \text{ cm}^2/\text{Vs}$  and  $\gamma = 1.6$  for the 10CuTBTAP OTFT. **As shown in Figure 4, the contact voltage  $V_S$  varies between 0 and -40 V. The value  $V_S = -20 \text{ V}$  used in (4) can be considered as the average value.** The solid lines are linear fittings in which the inverse of the slope determine the value of the contact resistance as a function of the gate voltage:  $R(0 \text{ V}) = 7.5 \times 10^8 \Omega$ ,  $R(-10 \text{ V}) = 7.5 \times 10^8 \Omega$ ,  $R(-20 \text{ V}) = 8.6 \times 10^8 \Omega$ ,  $R(-30 \text{ V}) = 9.9 \times 10^8 \Omega$ , and  $R(-40 \text{ V}) = 9.9 \times 10^8 \Omega$ , for the 10CuPc OTFT; and  $R(0 \text{ V}) = 11.3 \times 10^8 \Omega$ ,  $R(-10 \text{ V}) = 6.1 \times 10^8 \Omega$ ,  $R(-20 \text{ V}) = 5.4 \times 10^8 \Omega$ ,  $R(-30 \text{ V}) = 5.7 \times 10^8 \Omega$ ,  $R(-40 \text{ V}) = 5.5 \times 10^8 \Omega$ ,  $R(-50 \text{ V}) = 4.9 \times 10^8 \Omega$ , for the 10CuTBTAP OTFT. Introducing the values of all these parameters in the compact model (2), including the contact effects (6), the solid lines of Figure 5 are obtained. A good agreement with the experimental data is achieved.

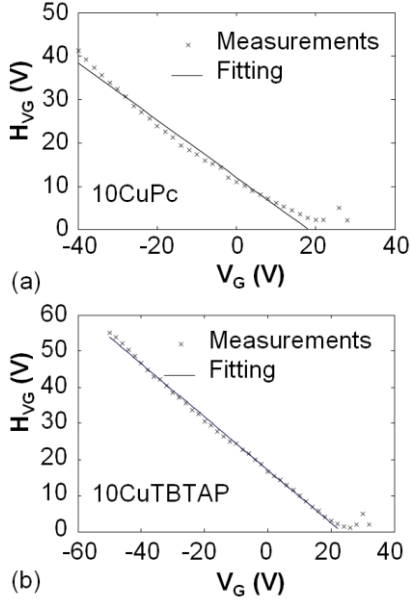


Fig. 3.  $H_{V_G}$  function extracted from transfer characteristics measured at  $V_D = -45$  V in (a) 10CuPc and (b) 10CuTBTAP OTFTs (symbols). The solid line is the fitting with (4) using  $V_T + V_S = 18$  V and  $\gamma = 1.5$  for the 10CuPc OTFT and  $V_T + V_S = 23$  V and  $\gamma = 1.6$  for the 10CuTBTAP case.

In order to show the sensitivity of the method, we consider different values of  $k_o$  in both transistors and determine the new  $I_D - V_S$  relation from (5). Maintaining the values of  $V_T$ ,  $V_S$ , and  $\gamma$  in each transistor but exchanging the values of  $\mu_o$  of both transistors, the resulting  $I_D - V_S$  curves are depicted in Figure 6. We observe how the  $I_D - V_S$  relations move away from a linear trend losing their physical meaning. A similar situation can be observed when the values of other parameters are changed.

#### IV. DISCUSSION

The results of the electrical characterization show that the threshold voltage in both transistors is very similar but the charge-carrier mobility in the 10CuPc material is four times as much as in the 10CuTBTAP material. The drain current does not follow the same relation as the mobility, being smaller in the 10CuPc transistor for gate voltages  $|V_G| > 10$  V. Only at gate voltages  $|V_G| < 10$  V, the drain current is higher in the material with higher mobility. The reason of this behavior is explained with the contact effects. On average, the contact voltage is around -20 V in both transistors, as seen in Figure 4. This average value has been useful as a way to determine the rest of the parameters of the model, in particular the values of the contact resistance extracted from the slope of the  $I_D - V_C$  curves at the contacts. The contact resistance is higher in the 10CuPc transistor and increases with the gate voltage. This makes the current density to be smaller, despite having obtained a higher mobility in the 10CuPc transistor. The high effect of the contact on the drain current for the 10CuPc transistors clearly opposes the effect of a higher mobility. The analysis of the experimental data with the ideal MOS model shows that the mobility is higher in the 10CuTBTAP transistor. With the ideal model, the mobility and the threshold voltage

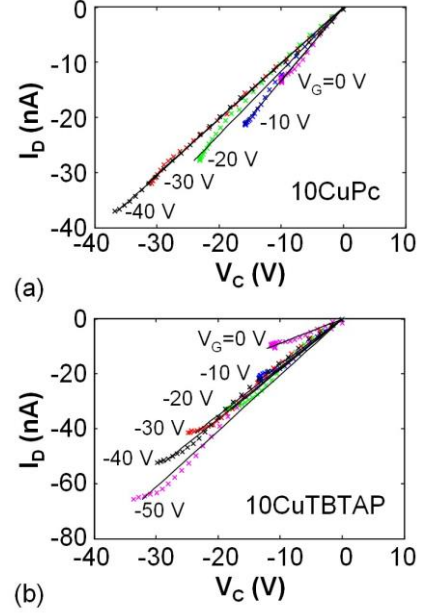


Fig. 4. Current voltage curves at the contact extracted from (5) using the experimental output characteristics at different gate voltages and the parameters (a)  $V_T = 38$  V,  $V_S = -20$  V,  $\mu_o = 7.2 \times 10^{-8}$  cm<sup>2</sup>/Vs and  $\gamma = 1.5$  for the 10CuPc OTFT and (b)  $V_T = 43$  V,  $V_S = -20$  V,  $\mu_o = 2.2 \times 10^{-8}$  cm<sup>2</sup>/Vs and  $\gamma = 1.6$  for the 10CuTBTAP OTFT. The solid lines are linear fittings that provide the value of the contact resistance.

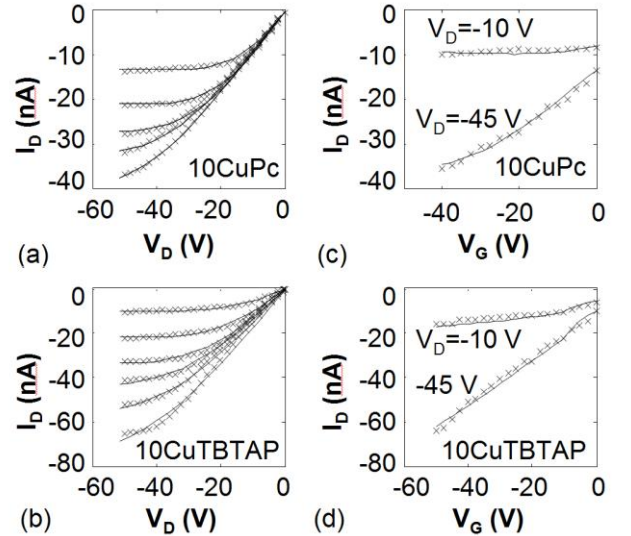


Fig. 5. Comparison of measured output characteristics [(a), (b)] and measured transfer characteristics [(c), (d)] in 10CuPc and 10CuTBTAP OTFTs (x) with the compact model (2) (solid lines). The calculations include the contact effects and the values of the parameters shown in Figure 4.  $V_G$  is swept from 0 to -40 V with a -10 V step in (a) and from 0 to -50 V with a -10 V step in (b), from top to bottom.

are the only parameters that allow interpreting the higher value of the current density in this transistor in comparison with the 10CuPc one. However, we have seen that the inclusion of the contact effects can reverse this conclusion and obtain a lower value of the mobility despite the higher current densities.

A further discussion about the values of the contact resistance can be made if we consider the variables it depends on. The contact resistance is proportional to the mobility  $\mu$  and

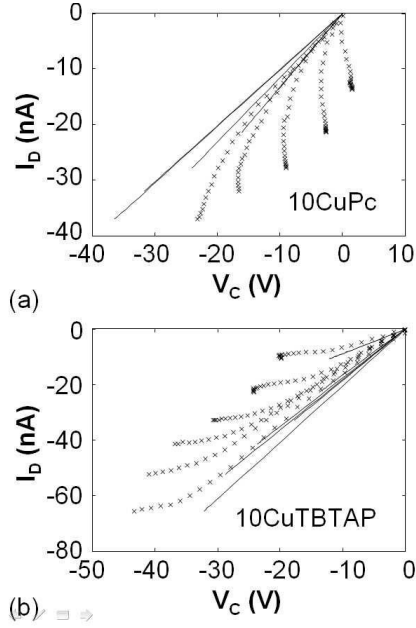


Fig. 6. Current voltage curves at the contact extracted from (5) using the experimental output characteristics at different gate voltages and the parameters (a)  $V_T = 38$  V,  $V_S = -20$  V,  $\mu_o = 2.2 \times 10^{-8}$  cm<sup>2</sup>/Vs and  $\gamma = 1.5$  for the 10CuPc OTFT and (b)  $V_T = 43$  V,  $V_S = -20$  V,  $\mu_o = 7.2 \times 10^{-8}$  cm<sup>2</sup>/Vs and  $\gamma = 1.6$  for the 10CuTBtAP OTFT. The solid lines are the linear fittings of Figure 4.

the charge volume density  $p_{contact}$  in this region:

$$1/R_C = qSp_{contact}\mu/x_C = \sigma_{contact}w\mu/x_C \quad (8)$$

where  $S$  is the cross section of the channel where current  $I_D$  flows,  $x_C$  is the contact length and  $\sigma_{contact}$  is free-charge surface density. The cause of the low conductivity of the contact region can thus be attributed to a lower mobility or a lower charge density in comparison to those at the intrinsic channel of the transistor. In [30], the path that the current follows from the contact towards the conducting channel is modeled with lower mobility, attributed to an anisotropic mobility.

The parameter  $R_C$  is expected to depend on the gate voltage, as many experiments have shown the dependence of the  $I_D - V_C$  curve at the contacts with the gate voltage [16], [17], [31]. To describe this dependence, we analyze the two regions of different conductivity distinguished along the channel of the organic transistor [23], [32], [33]: the low conductivity region close to the contact defined by the free-charge surface density  $\sigma_{contact} = x_C/(w\mu R_C)$  and the high conductivity region in the intrinsic channel defined by its counterpart free-charge surface-density, usually expressed as [34]  $\sigma_{channel} = C_A(V_G - V_T)$ . The free charge density in the contact region can be considered as a fraction of the last one:  $\sigma_{contact} = \sigma_{channel}/K$ . Although  $K$  is an undetermined constant, there is no physical reason to believe that the mobile charges in these two adjacent regions start appearing at very different gate voltages, or follow very different trends, unless local nonuniformities were present just at the contact region. Therefore,  $\sigma_{contact}$  can be assumed proportional to  $(V_G - V_T)$ .

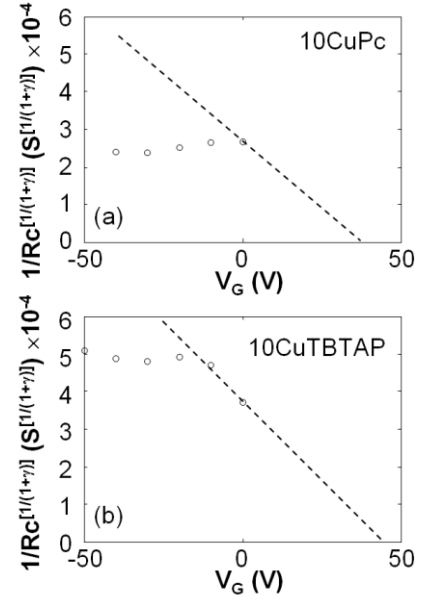


Fig. 7. Extracted values of  $1/R_C$  (circles). The dashed lines show the trend that  $1/R_C$  would follow according to (9). In the 10CuTBtAP case, the extrapolation of the data at low gate voltages intercepts with the  $V_G$ -axis at close to  $V_T = 43$  V. The deviation from this trend at more negative voltages can be explained by trapping effects inside the organic material.

Introducing this dependence and the gate voltage dependence of the mobility  $\mu = \mu_o(V_G - V_T)^\gamma$  in  $\sigma_{contact} = x_C/(w\mu R_C)$ , we can write

$$1/R_C = a_1(V_G - V_T)^{(1+\gamma)} \quad (9)$$

where  $a_1$  is a constant.

Figure 7 shows with circles the values of  $1/R_C$  obtained in the analysis of the 10CuPc and 10CuTBtAP transistors. The dashed lines show the trend that  $1/R_C$  should follow according to (9), in which the presence of local nonuniformities just at the contact region are ignored. In the 10CuPc transistor, the contact resistance is almost constant, not following (9). In the 10CuTBtAP transistor, the extrapolation of the data at low gate voltages intercept with the  $V_G$ -axis at close to  $V_T = 43$  V, following this trend. The deviation from this trend at more negative voltages can be explained by trapping effects inside the organic material. From this analysis, we can deduce that the 10CuPc transistor is highly affected by trapping in degradation induced defects. The 10CuTBtAP transistor, although not completely free of them, is less sensitive to these induced defects or traps.

## V. CONCLUSIONS

A comparative study between two organic thin film transistors fabricated with different organic materials (10CuPc and 10CuTBtAP) has been made with the aim of finding the best performance. Output and transfer characteristics have been measured in both transistors and a parameter extraction procedure has been used in order to determine the values of the threshold voltage, mobility and current-voltage curves at the contacts. A less precise procedure (ignoring contact

effects) has also been employed to determine the values of the mobility and threshold voltage. They point out the presence of anomalies. Nevertheless, they must be interpreted with more precise models. **In this regard, we highlight the analysis of the evolution of the contact resistance with the gate voltage. This analysis has been fundamental to detect more contact effects in the 10CuPc transistors produced not only by an increment of the contact resistance but also by the presence of more defects at the contact region, which can lead to a loss of stability in the OTFT.**

#### REFERENCES

- [1] D. M. Taylor, "Progress in organic integrated circuit manufacture," *Jpn. J. Appl. Phys.*, vol. 55, no. 2S, p. 02BA01, 2016.
- [2] C. Liao, M. Zhang, M. Y. Yao, T. Hua, L. Li, and F. Yan, "Flexible organic electronics in biology: Materials and devices," *Adv. Mater.*, vol. 27, no. 46, pp. 7493–7527, 2015.
- [3] Y. S. Rim, S.-H. Bae, H. Chen, N. De Marco, and Y. Yang, "Recent progress in materials and devices toward printable and flexible sensors," *Adv. Mater.*, vol. 28, no. 22, pp. 4415–4440, 2016.
- [4] M. Gsänger, D. Bialas, L. Huang, M. Stolte, and F. Würthner, "Organic semiconductors based on dyes and color pigments," *Adv. Mater.*, vol. 28, no. 19, pp. 3615–3645, 2016.
- [5] N. B. Chaure, A. N. Cammidge, I. Chambrier, M. J. Cook, M. G. Cain, C. E. Murphy, C. Pal, and A. K. Ray, "High-mobility solution-processed copper phthalocyanine-based organic field-effect transistors," *Sci. Technol. Adv. Mater.*, vol. 12, no. 2, p. 025001, 2011.
- [6] A. N. Cammidge, I. Chambrier, M. J. Cook, D. L. Hughes, M. Rahman, and L. Sosa-Vargas, "Phthalocyanine analogues: Unexpectedly facile access to non-peripherally substituted octaalkyl tetrabenzotriazaporphyrins, tetrabenzodiazaporphyrins, tetrabenzomonoazaporphyrins and tetrabenzoporphyrins," *Chem. Eur. J.*, vol. 17, no. 11, pp. 3136–3146, 2011.
- [7] Q.-D. Dao, K. Watanabe, H. Itani, L. Sosa-Vargas, A. Fujii, Y. Shimizu, and M. Ozaki, "Octahexyltetrabenzotriazaporphyrin: A discotic liquid crystalline donor for high-performance small-molecule solar cells," *Chem. Letts.*, vol. 43, no. 11, pp. 1761–1763, 2014.
- [8] Q.-D. Dao, L. Sosa-Vargas, T. Higashi, M. Ohmori, H. Itani, A. Fujii, Y. Shimizu, and M. Ozaki, "Efficiency enhancement in solution processed small-molecule based organic solar cells utilizing various phthalocyanine-tetrabenzoporphyrin hybrid macrocycles," *Org. Electron.*, vol. 23, pp. 44–52, 2015.
- [9] Y. Peng, W. Lv, B. Yao, J. Xie, T. Yang, G. Fan, D. Chen, P. Gao, M. Zhou, and Y. Wang, "Improved performance of photosensitive field-effect transistors based on palladium phthalocyanine by utilizing Al as source and drain electrodes," *IEEE Transactions on Electron Devices*, vol. 60, no. 3, pp. 1208–1212, March 2013.
- [10] N. B. Chaure, A. N. Cammidge, I. Chambrier, M. J. Cook, and A. K. Ray, "A tetrabenzotriazaporphyrin based organic thin film transistor: Comparison with a device of the phthalocyanine analogue," *ECS J. Solid State Sci. Technol.*, vol. 4, no. 4, pp. P3086–P3090, 2015.
- [11] O. Marinov, M. J. Deen, U. Zschieschang, and H. Klauk, "Organic thin-film transistors: Part I—compact dc modeling," *IEEE Trans. Electron Devices*, vol. 56, pp. 2952–2961, 2009.
- [12] M. J. Deen, O. Marinov, U. Zschieschang, and H. Klauk, "Organic Thin-Film Transistors: Part II. Parameter Extraction," *IEEE Trans. Electron Devices*, vol. 56, no. 12, pp. 2962–2968, Dec. 2009.
- [13] C. H. Kim, A. Castro-Carranza, M. Estrada, A. Cerdeira, Y. Bonnassieux, G. Horowitz, and B. Iniguez, "A compact model for organic field-effect transistors with improved output asymptotic behaviors," *IEEE Trans. Electron Devices*, vol. 60, no. 3, pp. 1136–1141, March 2013.
- [14] L. Li, M. Debucquoy, J. Genoe, and P. Heremans, "A compact model for polycrystalline pentacene thin-film transistor," *J. Appl. Phys.*, vol. 107, no. 2, p. 024519, 2010.
- [15] B. Yaglioglu, T. Agostinelli, P. Cain, S. Mijalkovi, and A. Nejm, "Parameter extraction and evaluation of uoftt model for organic thin-film transistor circuit design," *J. Disp. Technol.*, vol. 9, no. 11, pp. 890–894, Nov 2013.
- [16] D. J. Gundlach, L. Zhou, J. A. Nichols, T. N. Jackson, P. V. Necliudov, and M. S. Shur, "An experimental study of contact effects in organic thin film transistors," *J. Appl. Phys.*, vol. 100, no. 2, pp. 024 509–1–024509–13, 2006.
- [17] S. D. Wang, T. Minari, T. Miyadera, K. Tsukagoshi, and J. X. Tang, "Contact resistance instability in pentacene thin film transistors induced by ambient gases," *Appl. Phys. Lett.*, vol. 94, no. 8, pp. 083 309–1–083309–3, 2009.
- [18] M. J. Deen, M. H. Kazemeini, and S. Holdcroft, "Contact effects and extraction of intrinsic parameters in poly(3-alkylthiophene) thin film field-effect transistors," *J. Appl. Phys.*, vol. 103, no. 12, pp. 124 509–1–124509–7, 2008.
- [19] P. Lara Bullesjos, J. A. Jiménez Tejada, S. Rodríguez Bolívar, M. J. Deen, and O. Marinov, "Model for the injection of charge through the contacts of organic transistors," *J. Appl. Phys.*, vol. 105, no. 8, p. 084516, 2009.
- [20] J. A. Jiménez Tejada, J. A. López Villanueva, P. López Varo, K. M. Awawdeh, and M. J. Deen, "Compact modeling and contact effects in organic transistors," *IEEE Trans. Electron Devices*, vol. 61, no. 2, pp. 266–277, 2014.
- [21] Z. Xie, M. S. A. Abdou, X. Lu, M. J. Deen, and S. Holdcroft, "Electrical characteristics and photolytic tuning of poly(3-hexylthiophene) thin film metal-insulator-semiconductor field-effect transistors (misfets)," *Can. J. Phys.*, vol. 70, no. 10-11, pp. 1171–1177, Oct-Nov 1992, 6Th Canadian Semiconductor Technology Conf, Ottawa, Canada, Aug. 1992.
- [22] M. Deen, M. Kazemeini, Y. Haddara, J. Yu, G. Vamvounis, S. Holdcroft, and W. Woods, "Electrical characterization of polymer-based fets fabricated by spin-coating poly(3-alkylthiophene)s," *IEEE Trans. Electron Devices*, vol. 51, no. 11, pp. 1892–1901, Nov. 2004.
- [23] L. Bürgi, T. J. Richards, R. H. Friend, and H. Sirringhaus, "Close look at charge carrier injection in polymer field-effect transistors," *J. Appl. Phys.*, vol. 94, no. 9, pp. 6129–6137, 2003.
- [24] A. Cerdeira, M. Estrada, R. García, A. Ortiz Conde, and F. García Sánchez, "New procedure for the extraction of basic a-Si:H TFT model parameters in the linear and saturation regions," *Solid-State Electron.*, vol. 45, no. 7, pp. 1077–1080, 2001.
- [25] J. Jiménez Tejada, K. M. Awawdeh, J. A. López Villanueva, J. E. Carceller, M. J. Deen, N. B. Chaure, T. Basova, and A. K. Ray, "Contact effects in compact models of organic thin film transistors: Application to zinc phthalocyanine-based transistors," *Org. Electron.*, vol. 12, no. 5, pp. 832–842, 2011.
- [26] K. M. Awawdeh, J. A. Jiménez Tejada, P. López Varo, J. A. López Villanueva, F. M. Gómez Campos, and M. J. Deen, "Characterization of organic thin film transistors with hysteresis and contact effects," *Org. Electron.*, vol. 14, no. 12, pp. 3286–3296, 2013.
- [27] P. Lara Bullesjos, J. A. Jiménez Tejada, M. J. Deen, O. Marinov, and W. R. Datars, "Unified model for the injection and transport of charge in organic diodes," *J. Appl. Phys.*, vol. 103, no. 6, pp. 064 504–1–064504–12, 2008.
- [28] P. Lara Bullesjos, J. A. Jiménez Tejada, F. M. Gómez-Campos, M. J. Deen, and O. Marinov, "Evaluation of the charge density in the contact region of organic thin film transistors," *J. Appl. Phys.*, vol. 106, no. 9, pp. 094 503–1–094 503–4, 2009.
- [29] P. López Varo, J. Jiménez Tejada, J. López Villanueva, J. Carceller, and M. Deen, "Modeling the transition from ohmic to space charge limited current in organic semiconductors," *Org. Electron.*, vol. 13, no. 9, pp. 1700–1709, 2012.
- [30] C. W. Sohn, T. U. Rim, G. B. Choi, and Y. H. Jeong, "Analysis of contact effects in inverted-staggered organic thin-film transistors based on anisotropic conduction," *IEEE Trans. Electron Devices*, vol. 57, no. 5, pp. 986–994, 2010.
- [31] S. D. Wang, T. Minari, T. Miyadera, K. Tsukagoshi, and Y. Aoyagi, "Contact-metal dependent current injection in pentacene thin-film transistors," *Appl. Phys. Lett.*, vol. 91, no. 20, p. 203508, 2007.
- [32] C. H. Kim, Y. Bonnassieux, and G. Horowitz, "Charge distribution and contact resistance model for coplanar organic field-effect transistors," *IEEE Trans. Electron Devices*, vol. 60, no. 1, pp. 280–287, 2013.
- [33] Y. Ishikawa, Y. Wada, and T. Toyabe, "Origin of characteristics differences between top and bottom contact organic thin film transistors," *J. Appl. Phys.*, vol. 107, no. 5, pp. 053 709–1–053 709–7, 2010.
- [34] B. G. Streetman, *Solid State Electronic Devices*. Prentice-Hall, Englewood Cliffs, NJ, 1980.